

PAPER

Oleyamine-assisted and temperature-controlled synthesis of ZnO nanoparticles and their application in encryption

To cite this article: Shu-Li Wang *et al* 2019 *Nanotechnology* **30** 015702

View the [article online](#) for updates and enhancements.



IOP | ebooks™

Bringing you innovative digital publishing with leading voices to create your essential collection of books in STEM research.

Start exploring the collection - download the first chapter of every title for free.

Oleylamine-assisted and temperature-controlled synthesis of ZnO nanoparticles and their application in encryption

Shu-Li Wang^{1,2}, Kai-Kai Liu^{1,3,4}, Chong-Xin Shan^{1,3} , En-Shan Liu^{1,2} and De-Zhen Shen^{1,4}

¹ State Key Laboratory of Luminescence and Applications, Changchun Institute of Optics, Fine Mechanics and Physics, Chinese Academy of Sciences, Changchun, 130033, People's Republic of China

² University of Chinese Academy of Sciences, Beijing, 100049, People's Republic of China

³ Henan Key Laboratory of Diamond Optoelectronic Materials and Devices, School of Physics and Engineering, Zhengzhou University, Zhengzhou, 450052, People's Republic of China

E-mail: liukaikai@ciomp.ac.cn and shenzd@ciomp.ac.cn

Received 23 June 2018, revised 3 October 2018

Accepted for publication 5 October 2018

Published 25 October 2018



Abstract

A temperature-controlled synthesis process for ZnO nanoparticles (NPs) with the assist of oleylamine (OAm) has been demonstrated, and the ZnO NPs show bright fluorescence under ultraviolet illumination. In this process, zinc nitrate was firstly converted to zinc nitrate hydroxide ($Zn_5(OH)_8(NO_3)_2$) sheets with the assist of OAm, then the $Zn_5(OH)_8(NO_3)_2$ was decomposed into fluorescent ZnO NPs by increasing the ambient temperature. Furthermore, information encryption has been realized based on this process. For encryption, the encrypted information cannot be observed, while the encrypted information appears when they are proceeded in the temperature of 120 °C for about one minute. The results shown in this work provide a controllable way for the synthesis of ZnO NPs by adjusting the reaction temperature, and this may inspire wide applications of ZnO in information encryption.

Keywords: ZnO NPs, temperature-controlled synthesis, information encryption

(Some figures may appear in colour only in the online journal)

1. Introduction

Information security is of vital significance in many fields, including political activities, commercial activities, military communications and individual privacy. In the last few years, diverse functional materials [1–5] that are responsive to external stimuli have been developed for information recording, storage and encryption [6–8]. Fluorescent nanoparticles (NPs), as one of the most promising candidates, have been applied in the field of date recording, anti-counterfeiting and entity encryption [9–12]. Generally, fluorescent NPs are used as inks to produce patterns on various substrates, which is visible only in certain illumination conditions or chemical conditions [13–15]. For example, Ma *et al* have used

upconversion NPs (UCNPs) as inks [9]. The UCNPs can efficiently eliminate background fluorescence interference, and the printed information can only be visualized under NIR light excitation. However, the authors used upconversion rare-earth NPs as fluorescent inks, the serious environmental pollution problems limit their further applications in information encryption field. Deng *et al* have reported a fluorescent polyfluorene-containing methacrylate macromonomer (PFMA) and its well-defined copolymers with 2-(dimethylamino)ethyl methacrylate (DMAEMA) [P(PFMA-*r*-DMAEMA)*s*], and these copolymers self-assemble into photoluminescent NPs in aqueous solutions [11]. The highlight of their work is that they realized multicolor patterns on papers by using these solutions as inks. However, it is hard to be applied because of the potential biotoxicity of the organic materials. Han *et al* used CdSe/CdS/ZnS quantum dots (QDs) as fluorescent inks [15].

⁴ Authors to whom any correspondence should be addressed.

They designed a new dual functional group polymer, mercaptopropionic polyethylenimine (MPPEI), as a ligand combines the thiol of 3-mercaptopropionic acid (MPA) with the amine of polyethylenimine (PEI) for the surface functionalization of CdSe/CdS/ZnS QDs. The branched structure of MPPEI can provide QDs with very effective protection such as acid resistance, base resistance, photostability and thermostability. However, the Cd^{2+} will not only pollute the environment but also be harmful to the health of human beings. Zhang *et al* used carbon nanodots as inks [14]. The low-cost, eco-friendly and easily prepared carbon nanodots can be applied in the field of information encryption. However, this method is too simple, and it is easy to be cracked. These methods have been widely known to people, thus the encrypted information can be easily cracked. An alternative method to information encryption is to switch single-luminophore liquid crystal to tricolored luminescence by mechanical stimuli [16]. However, because of the low photostability, potential biological toxicity of the functional materials and complex process of these methods, their application in the field of entity encryption are limited. Therefore, it is still of great significance to develop simple and controllable process for information encryption.

In recent years, ZnO NPs have attracted increasing attention for their unique photoelectric and low-cost, eco-friendly, and easy synthesis characters. ZnO have been widely applied in bioimaging [17–19], photocatalysis [20–22], ultraviolet photodetectors [23–25], light-emitting diodes [26–28], spin electric devices [29, 30], solar cells [31, 32], and gas sensors [33, 34], etc. Additionally, ZnO NPs are extremely responsive to some specific external stimuli, which have achieved great applications in many fields. In our previous work, pH-sensitive ZnO NPs have been synthesized, and the ZnO NPs have been used for rewritable painting and advanced encryption based on the fluorescence quenching in different conditions [35, 36]. However, the synthesis process of ZnO NPs cannot be controlled and the ZnO NPs will be formed within several minutes. Therefore, developing simple and controllable process for ZnO NPs is still a challenge.

In this paper, a temperature-controlled synthesis process for ZnO NPs has been developed with the assist of OAm, and the ZnO NPs have been applied for information encryption. In this process, $\text{Zn}(\text{NO}_3)_2 \cdot 6\text{H}_2\text{O}$ was converted into $\text{Zn}_5(\text{OH})_8(\text{NO}_3)_2$ sheets with the assist of OAm, then fluorescent ZnO NPs were grown on the surface of the $\text{Zn}_5(\text{OH})_8(\text{NO}_3)_2$ by adjusting the ambient temperature. The formation of ZnO NPs from $\text{Zn}_5(\text{OH})_8(\text{NO}_3)_2$ sheets can be controlled by the reaction temperature, thus this process can be used for encryption due to the different fluorescence characters of the $\text{Zn}_5(\text{OH})_8(\text{NO}_3)_2$ sheets and ZnO NPs. This work provides a controllable way for synthesis ZnO NPs, and this may inspire wide applications of ZnO NPs in information encryption.

2. Experimental sections

2.1. Chemicals

The reagents used in this experiment were zinc nitrate hexahydrate ($\text{Zn}(\text{NO}_3)_2 \cdot 6\text{H}_2\text{O}$, purity > 99%), OAm ($\text{CH}_3(\text{CH}_2)_7\text{CH}=\text{CH}(\text{CH}_2)_7\text{CH}_2\text{NH}_2$), deionized water and ethanol (purity > 99%). All the chemical reagents were used as received without further purification.

2.2. Preparation of ZnO NPs

The preparation procedures of the ZnO NPs were as follows: firstly, 6.6 g $\text{Zn}(\text{NO}_3)_2 \cdot 6\text{H}_2\text{O}$ were dissolved in 110 ml deionized water under vigorous stirring at room temperature for 5 min until the solution became pellucid. Secondly, 6 ml of OAm were added into the above solution. Immediately, the solution turned turbid and it means that the $\text{Zn}_5(\text{OH})_8(\text{NO}_3)_2$ sheets had been formed. After 15 min continuous stirring, the reaction was finished entirely and the solution became milky. Thirdly, the turbid solution was centrifuged (5000 rpm, 3 min) and the obtained $\text{Zn}_5(\text{OH})_8(\text{NO}_3)_2$ precipitates were washed with ethanol for several times to remove the unreacted precursors, and the precipitates were placed into lyophilizer for 5 h. Then the dry solid powders of non-fluorescent $\text{Zn}_5(\text{OH})_8(\text{NO}_3)_2$ were obtained. Finally, the precipitates were put into ovens at different temperatures from 70 °C to 150 °C at 10 °C intervals for 15 min, respectively. The obtained products were stored in a box for further study and application. At 80 °C, the $\text{Zn}_5(\text{OH})_8(\text{NO}_3)_2$ began to form to ZnO NPs. From 80 °C to 110 °C, the milky solid is the mixture of $\text{Zn}_5(\text{OH})_8(\text{NO}_3)_2$ sheets and ZnO NPs. Above 110 °C, the milky solid are most of ZnO NPs.

2.3. Application in encryption

Firstly, the $\text{Zn}(\text{NO}_3)_2 \cdot 6\text{H}_2\text{O}$ aqueous solution was injected into the cartridge of a printer (HP-1510) as ink. Then the cartridge was put into the printer, and certain images were printed onto copy papers by the printer. After that, OAm alcohol solution was sprayed onto the papers, and this is a liquid reaction process. Finally, these papers were put into an oven and heated at 120 °C for different times, and this is the solid state reaction. It is worth mentioning that the paper used in this experiment was non-fluorescent so that it had no interference to the encrypted information under UV lighting condition. Besides, the paper should have a degree of water absorbing capacity, because the $\text{Zn}(\text{NO}_3)_2 \cdot 6\text{H}_2\text{O}$ aqueous solution was injected into the cartridge of a printer as ink to print patterns on the paper.

2.4. Characterizations

The structural properties of the precipitates and ZnO NPs were characterized by a JEM-2010 transmission electron microscope (TEM) and a S-4800 scanning electron microscope (SEM). The chemical phases of the samples were

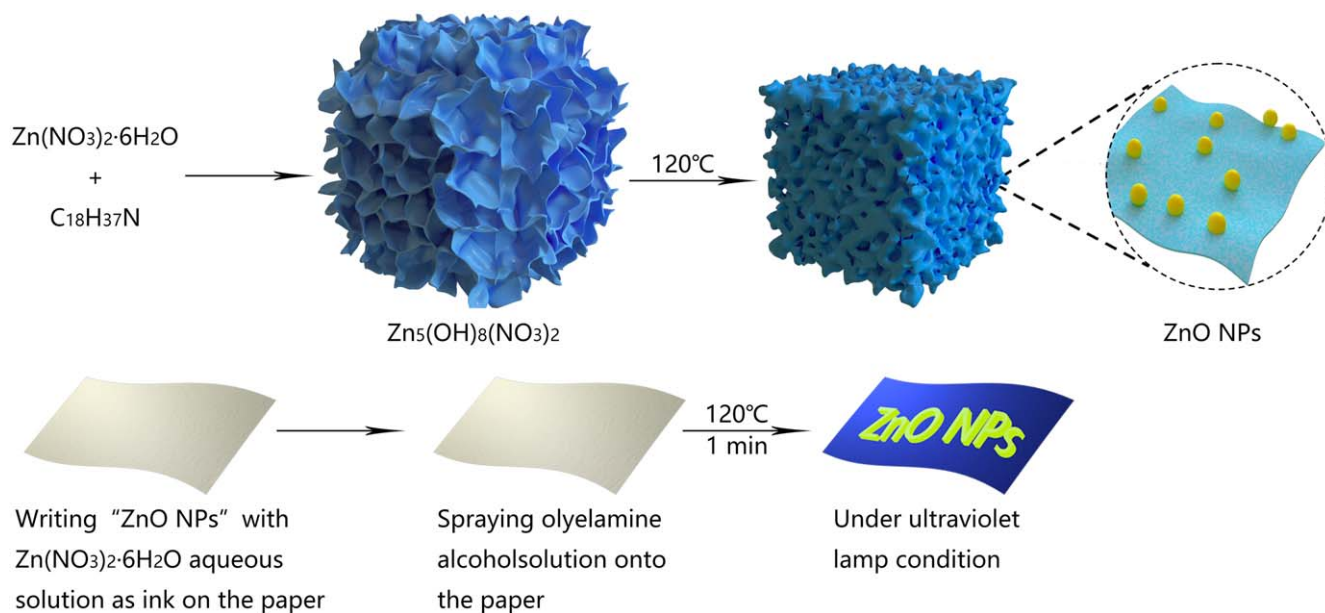


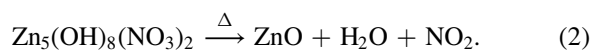
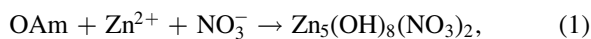
Figure 1. Schematic illustration of the temperature-controlled synthesis process of ZnO NPs.

measured by a D-8 focus x-ray diffractometer. The radicals of the samples were characterized using a Bruker VERTEX-70 Fourier transform infrared (FTIR) spectrometer. The fluorescence properties of the samples were recorded in a Hitachi F-7000 spectrometer. The absorption spectra of the samples were acquired on a Shimadzu UV-3101PC spectrometer. The transient photoluminescence spectra of the ZnO NPs were collected on a FLS-920 fluorescence spectrometer.

3. Results and discussion

3.1. Morphology and structure of the $Zn_5(OH)_8(NO_3)_2$ and ZnO NPs

The ZnO NPs were synthesized in two steps: firstly, precursor $Zn(NO_3)_2 \cdot 6H_2O$ hydrolyzed into $Zn_5(OH)_8(NO_3)_2$ with the assistance of OAm. Then the $Zn_5(OH)_8(NO_3)_2$ dehydrated into ZnO NPs with increase the temperature. The corresponding reaction equations are as follows:



The main role of OAm is that precursor $Zn(NO_3)_2 \cdot 6H_2O$ can hydrolyze into intermediate product $Zn_5(OH)_8(NO_3)_2$ with the assistance of amidogen from OAm, and then the $Zn_5(OH)_8(NO_3)_2$ dehydrated into ZnO NPs with increase of temperature. Figure 1 shows the synthesis process of the $Zn_5(OH)_8(NO_3)_2$ and ZnO NPs and their application in information encryption. The $Zn_5(OH)_8(NO_3)_2$ is prepared by amino of OAm provides an alkaline environment so that $Zn(NO_3)_2 \cdot 6H_2O$ can hydrolyze into $Zn_5(OH)_8(NO_3)_2$. At 120 °C, the $Zn_5(OH)_8(NO_3)_2$ can be dehydrated into fluorescent ZnO NPs. The SEM and TEM images of the $Zn_5(OH)_8(NO_3)_2$ at 25 °C, 110 °C, 130 °C and 150 °C are shown in figure 2. It can be seen from figures 2(a1) and (a2)

that the sample synthesized at 25 °C has sheet-like structure. When the $Zn_5(OH)_8(NO_3)_2$ sheets were heated at 110 °C, the structure shrinks obviously, and some spherical dots can be seen clearly on the surface of the sheets, as shown in figures 2(b1) and (b2). With further increase of temperature, the sheets become thicker, and more and more dots can be observed on the surface of the sheets, as shown in figures 2(c1), (c2), (d1), and (d2). The average particle size of the dots is 5.3 nm, as indicated in the inset of figure 2(c2). The $Zn_5(OH)_8(NO_3)_2$ has clear lattice fringes with a spacing of about 0.27 nm, which corresponds to the distance of (021) planes of $Zn_5(OH)_8(NO_3)_2$, as shown in figure 2(a3) and inset. The clear lattice fringes of the ZnO NPs with a spacing of about 0.26 nm can be observed, which corresponds to the distance of (002) planes of ZnO, as indicated in figure 2(b3) and inset. Figures 2(c3) and (d3) also present the crystallinity of the ZnO NPs when the ambient temperature increases to 150 °C.

To further exploit the forming mechanism of the ZnO NPs, x-ray diffraction (XRD) patterns of the sheets heated at various temperatures for 15 min were recorded, as shown in figure 3(a). The diffraction peaks of the sheets at 25 °C match well with that of zinc nitrate hydroxide, indicating the product is $Zn_5(OH)_8(NO_3)_2$. The XRD patterns of the samples change little until they were heated at 70 °C, indicating that the $Zn_5(OH)_8(NO_3)_2$ is stable when temperature is below 70 °C. A diffraction peak appears at about 36° when temperature is increased to 80 °C, and the diffraction peak corresponds to the diffraction of (101) face of ZnO, indicating that ZnO NPs have been formed. From the XRD patterns of the samples heated in the temperature range from 90 °C to 110 °C, $Zn_5(OH)_8(NO_3)_2$ and ZnO NPs coexist. When the samples are heated at temperature above 110 °C, the diffraction peaks of the $Zn_5(OH)_8(NO_3)_2$ disappear, indicating that most of the $Zn_5(OH)_8(NO_3)_2$ have been converted to ZnO.

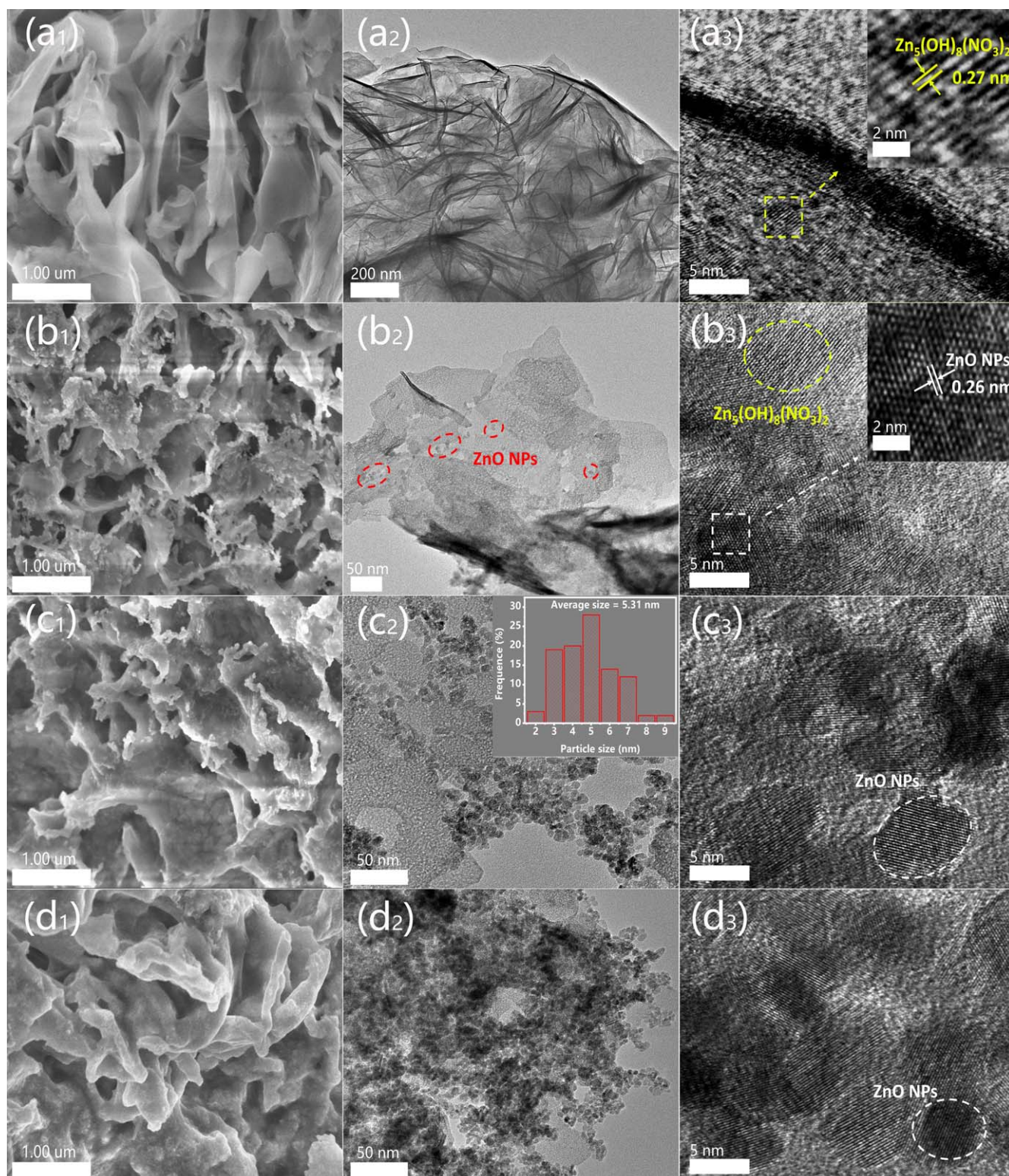


Figure 2. (a1) The SEM, (a2) TEM and (a3) HRTEM images of the samples at 25 °C. (b1) SEM, (b2) TEM and (b3) HRTEM images of the sample treated at 110 °C for 15 min (c1) SEM, (c2) TEM and (c3) HRTEM images of the sample treated at 130 °C for 15 min, and inset shows the size distribution of the ZnO NPs. (d1) SEM, (d2) TEM and (d3) HRTEM images of the samples treated at 150 °C for 15 min.

In order to characterize the surface functional groups of the $\text{Zn}_5(\text{OH})_8(\text{NO}_3)_2$, FTIR spectra of the samples have been recorded, as indicated in figure 3(b). The broadband at around 3447 cm^{-1} belongs to the stretching vibration of O–H and the peak at about 1632 cm^{-1} belongs to the bending vibration of

O–H, and both of them are from absorbed water molecules. The peaks at 2920 and 2850 cm^{-1} represent the methyl and methylene stretching vibration of C–H, and the peak at 1030 cm^{-1} belongs to the stretching vibration of C–O. Both the bond of the C–H and C–O come from the residual OAm.

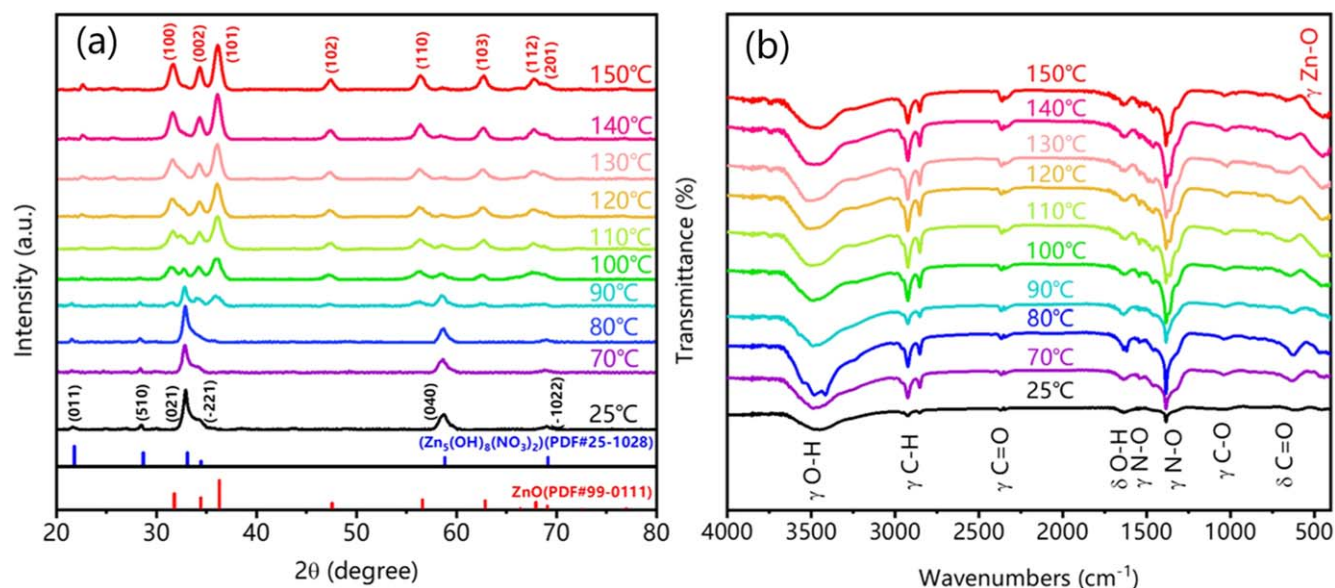


Figure 3. (a) X-ray diffraction patterns and (b) FTIR spectra of the samples treated for 15 min at different temperatures.

The peaks at around 1540 and 1382 cm^{-1} are from the stretching vibration of N–O. At 80°C , the peak centered at 438 cm^{-1} belongs to the stretching vibration absorption of Zn–O bond [37]. The above results indicate that the critical temperature beginning to form ZnO NPs is at 80°C , which is consistent with the XRD results.

3.2. Optical properties of the ZnO NPs

Figure 4(a) shows the absorption spectra of the samples heated at different temperatures. The absorption spectra of the $\text{Zn}_5(\text{OH})_8(\text{NO}_3)_2$ are located at around 270 nm , and no changes can be observed until temperature increases to 70°C . An absorption peak at around 365 nm appears when the temperatures are in the range from 80°C to 150°C , indicating that ZnO NPs have been formed. It can be concluded from the above results that ZnO NPs are formed gradually when temperature is above 80°C .

The fluorescence spectra of the samples heated at different temperatures have been measured, as shown in figure 4(b). In figure 4(b), no obvious emission can be observed when the $\text{Zn}_5(\text{OH})_8(\text{NO}_3)_2$ powder was processed at 25°C , 70°C and 80°C . While all the spectra are dominated by a broad emission at around 548 nm when they are heated in the range from 90°C to 150°C , which can be attributed to the defect-related emission of ZnO. For clarity, the variation of the fluorescence intensity versus temperature has been plotted, as shown in figure 4(c), and the fluorescence images of the powder are also illustrated in the inset of figure 4(c). Obvious fluorescence can be observed from the samples when they are heated at 90°C , and the intensity increases gradually with the treatment temperature, while when the temperature is above 110°C , the fluorescence intensity decreases significantly. The above trend can be understood as follows: with the increase of treatment temperature, more and more fluorescent ZnO NPs are formed, thus the fluorescence intensity of the sample increased, while when the treatment temperature is

above 110°C , the crystalline quality of the ZnO NPs becomes better, thus the deep-level related emission decreased.

To assess the effect of the treatment duration on the fluorescence of the samples, the fluorescence spectra of the samples treated for 5, 10, 15, 20, and 25 min at 120°C are illustrated in figure 4(d). It can be seen that the emission intensity of the ZnO NPs reaches its maximum when they are heated for 10 min, while the intensity decreases with further increasing the treatment time, as shown in figure 4(d). The reason of increasing fluorescent intensity initially can be attributed to the continuous growth of the fluorescent ZnO NPs, while with further increase in the treatment duration, the crystalline quality of the ZnO NPs will be improved, thus the deep-level defects' emission decreased.

To explore the carrier recombination process in the ZnO NPs, the transient spectra of the emission at 548 nm are illustrated in figure 4(e), which can be well fitted using the following two-order exponential decay formula:

$$y = y_0 + A_1 \exp(-t/\tau_1) + A_2 \exp(-t/\tau_2), \quad (3)$$

where y is the emission intensity, t is time, y_0 , A_1 , A_2 are constant, and τ_1 and τ_2 are lifetime of the emission. The results are shown in table 1.

τ_1 may come from the deep-level recombination inside the ZnO NPs, while τ_2 may come from the surface defects [38]. The different samples have the similar lifetime of τ_1 and τ_2 , indicated the same carrier recombination process of ZnO NPs heated for different times at 120°C .

3.3. Application in encryption

As discussed above, with the assist of OAm, precursor zinc nitrate can be converted to non-fluorescent $\text{Zn}_5(\text{OH})_8(\text{NO}_3)_2$ sheet. Since zinc nitrate can hydrolyze easily in a weakly alkaline environment, and OAm can provide weak alkaline environment to assist the synthesis of non-fluorescent $\text{Zn}_5(\text{OH})_8(\text{NO}_3)_2$ sheet. The reaction equation is shown in

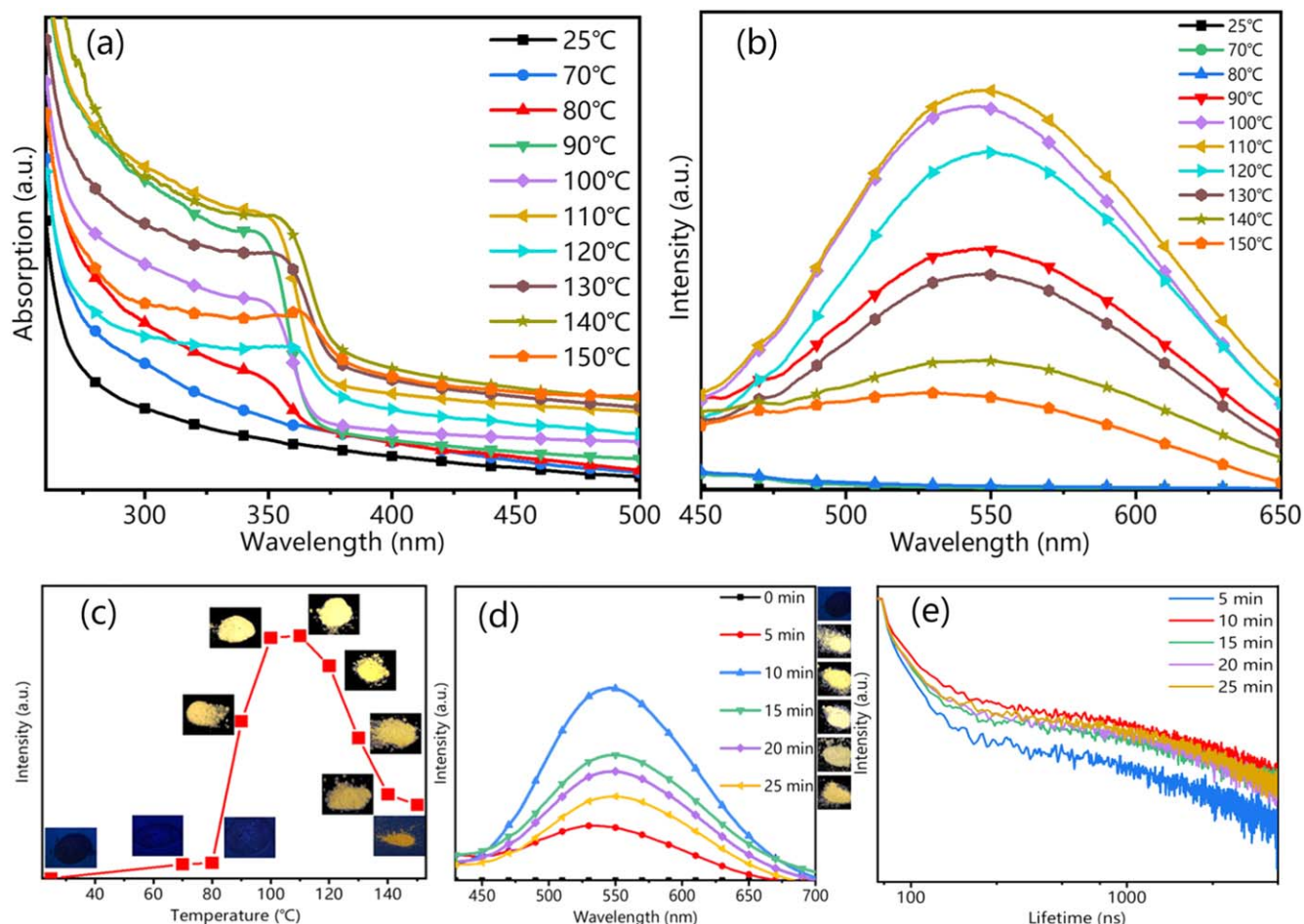


Figure 4. (a) Absorption spectra of the samples treated for 15 min at different temperatures. (b) The fluorescence spectra of the samples treated for 15 min at different temperatures. (c) The dependence of the fluorescence intensity on the treatment temperature. (d) The fluorescence spectra of the samples treated at 120 °C for different times. (e) Transient photoluminescence spectra of the samples treated at 120 °C for different times.

Table 1. The lifetime of the ZnO NPs at different treatment durations.

	5 min	10 min	15 min	20 min	25 min
τ_1 (ns)	14.40	21.45	17.00	17.46	17.35
τ_2 (ns)	687.82	1024.43	973.44	1044.68	1150.53

equation (1) above. Then, the non-fluorescent $Zn_5(OH)_8(NO_3)_2$ sheets can be dehydrated into fluorescent ZnO NPs easily by increase the ambient temperature, and the reaction equation is shown in equation (2) above. Using the above process, an encryption process has been proposed. For encryption, the encrypted logo of 'CIOMP' was printed onto a phosphor-free copy paper using $Zn(NO_3)_2 \cdot 6H_2O$ aqueous solution as ink. The patterns cannot be seen under UV and indoor lighting conditions because of the non-fluorescence and colorless of the solution. In the next step, alcohol solution with OAm was sprayed onto the logo, and the zinc nitrate on paper immediate becomes non-fluorescent $Zn_5(OH)_8(NO_3)_2$ with the assist of OAm due to the reaction between $Zn(NO_3)_2 \cdot 6H_2O$ and OAm. At this stage, the encrypted logo still cannot be observed. For decryption, the paper with encrypted logo was put into an oven

with temperature of 120 °C for 1 min, 2 min, 5 min, 10 min, 15 min, 20 min and 60 min, respectively. The encrypted logo can be observed clearly even when the paper was heated for only 1 min, indicating the decrypted process can be performed quickly. The paper with encrypted logo heated for different times is shown in figure 5(a), and the inset is the original image. One can see that all the encrypted logos can be observed clearly under UV illumination, and the emerging of the logos can be attributed to the formation of the fluorescent ZnO NPs. To further evaluate the fidelity of the decrypted patterns, the decrypted patterns have been analyzed using MATLAB. The average gray values of eight images shown in figure 5(a) have been calculated, as shown in figure 5(b). The gray values of the patterns reach their maximum when the patterns are heated at 120 °C for 10 min, because ZnO NPs show the strongest fluorescence at this condition. The gray values of the patterns heated for 0, 1 and 10 min in figure 5(a) along the red dashed lines have been extracted, as indicated in figure 5(c). The gray level of the encrypted pattern (0 min) along the red dash line is almost constant, which means that the pattern has been hidden and encrypted well. While the gray values of the decrypted patterns show the same variations compared with those of the original image, which indicates that

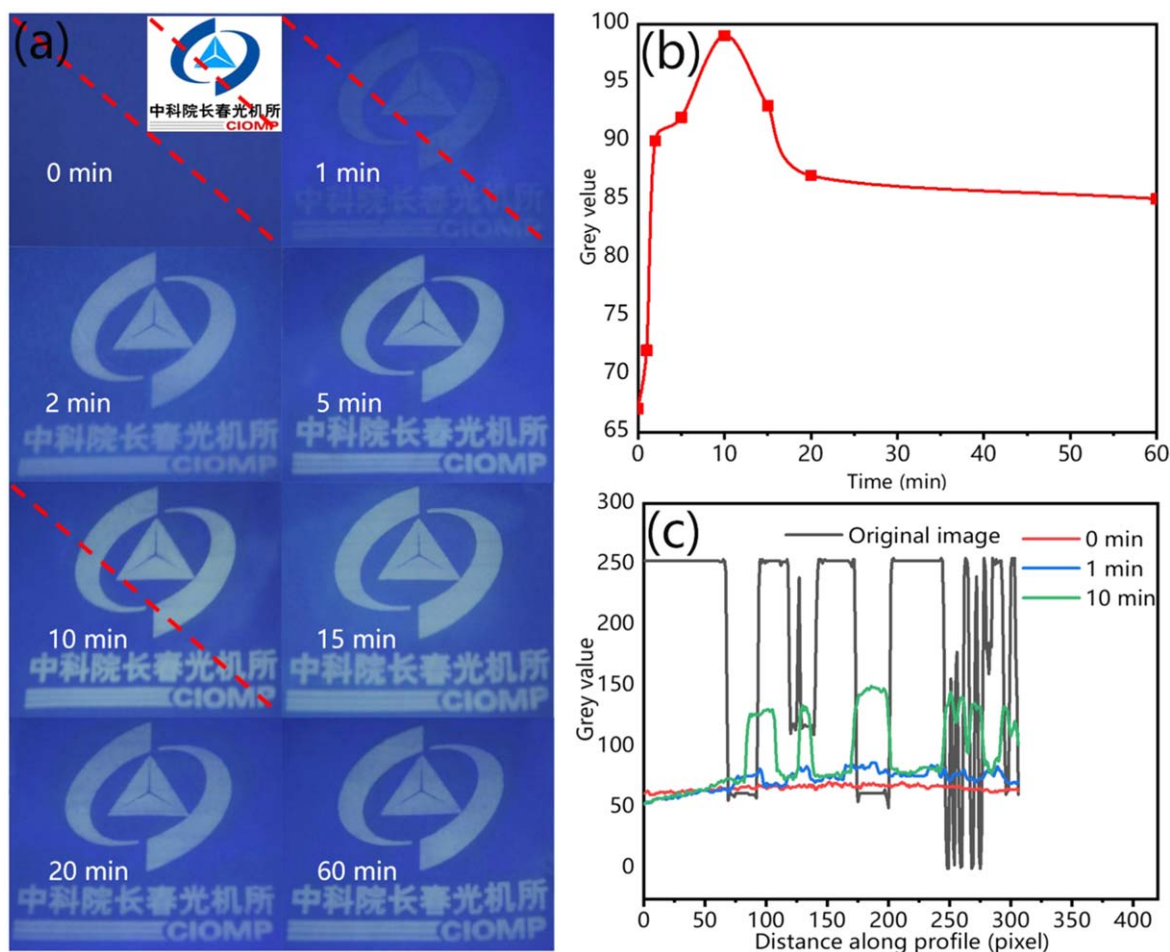


Figure 5. (a) The encrypted logos of 'CIOMP' treated at 120 °C for different times, and the inset is the original image of the logo. (b) The average gray values of the logos in (a). (c) The variations of gray values along the red dash lines in (a).

the decrypted patterns match the original images well, which provides a promising application for the fields of information encryption.

4. Conclusions

In conclusion, a temperature-controlled synthesis process for ZnO NPs has been realized with the assist of OAm. $Zn_5(OH)_8(NO_3)_2$ sheets were formed firstly when the $Zn(NO_3)_2 \cdot 6H_2O$ precursor was reacted with OAm, then ZnO NPs will grow on the surface of the $Zn_5(OH)_8(NO_3)_2$ sheets by adjusting the treatment temperature. Furthermore, a simple strategy for information encryption has been developed in view of the controllable process. For encryption, the encrypted information cannot be observed under UV or indoor lighting conditions, while for decryption, the encrypted patterns appear under UV lighting condition when they are treated at 120 °C. The results reported in this paper may find potential applications in information security in the future.

Acknowledgments

This work is financially supported by the National Science Foundation for Distinguished Young Scholars of China (61425021), the Natural Science Foundation of China (61604132 and U1604263).

ORCID iDs

Chong-Xin Shan  <https://orcid.org/0000-0001-9312-6486>

References

- [1] Zhou P, Chen L, Yao L, Weng M and Zhang W 2018 Humidity- and light-driven actuators based on carbon nanotube-coated paper and polymer composite *Nanoscale* **10** 8422–7
- [2] Zhang B, Kowsari K, Serjouei A, Dunn M L and Ge Q 2018 Reprocessable thermosets for sustainable three-dimensional printing *Nat. Commun.* **9** 1831

- [3] Zhang T, Li K, Zhang J, Chen M, Wang Z, Ma S, Zhang N and Wei L 2017 High-performance, flexible, and ultralong crystalline thermoelectric fibers *Nano Energy* **41** 35–42
- [4] Peng C, Chen Z and Tiwari M K 2018 All-organic superhydrophobic coatings with mechanochemical robustness and liquid impalement resistance *Nat. Mater.* **17** 355–60
- [5] Kamihara Y, Watanabe T, Hirano M and Hosono H 2008 Iron-based layered superconductor $\text{La}[\text{O}_{1-x}\text{F}_x]\text{FeAs}$ ($x = 0.05\text{--}0.12$) with $T_c = 26$ K *J. Am. Chem. Soc.* **130** 3296–7
- [6] Hu J et al 2007 A non-planar organic molecule with non-volatile electrical bistability for nano-scale data storage *J. Mater. Chem.* **17** 3530
- [7] Jiang G, Wang S, Yuan W, Jiang L, Song Y, Tian H and Zhu D 2006 Highly fluorescent contrast for rewritable optical storage based on photochromic bisthienylethene-bridged naphthalimide dimer *Chem. Mater.* **18** 235–7
- [8] Elgemeie G H, Ahmed K A, Ahmed E A, Helal M H and Masoud D M 2016 A simple approach for the synthesis of coumarin fluorescent dyes under microwave irradiation and their application in textile printing *Pigm. Resin Technol.* **45** 217–24
- [9] Ma Q, Wang J, Li Z, Wang D, Hu X, Xu Y and Yuan Q 2017 Near-infrared-light-mediated high-throughput information encryption based on the inkjet printing of upconversion nanoparticles *Inorg. Chem. Front.* **4** 1166–72
- [10] You M, Lin M, Wang S, Wang X, Zhang G, Hong Y, Dong Y, Jin G and Xu F 2016 Three-dimensional quick response code based on inkjet printing of upconversion fluorescent nanoparticles for drug anti-counterfeiting *Nanoscale* **8** 10096–104
- [11] Deng C, Yang Z, Zheng Z, Liu N and Ling J 2015 Photoluminescent nanoparticles in water with tunable emission for coating and ink-jet printing *J. Mater. Chem. C* **3** 3666–75
- [12] Sandhyarani A, Kokila M K, Darshan G P, Basavaraj R B, Daruka Prasad B, Sharma S C, Lakshmi T K S and Nagabhushana H 2017 Versatile core-shell $\text{SiO}_2@\text{SrTiO}_3$: Eu^{3+} , Li^+ nanopowders as fluorescent label for the visualization of latent fingerprints and anti-counterfeiting applications *Chem. Eng. J.* **327** 1135–50
- [13] Bao B, Li M, Li Y, Jiang J, Gu Z, Zhang X, Jiang L and Song Y 2015 Patterning fluorescent quantum dot nanocomposites by reactive inkjet printing *Small* **11** 1649–54
- [14] Zhang X T, Li D, Zhou D, Jing P T, Ji W, Shen D Z and Qu S N 2016 Dual-encryption based on facilely synthesized supra-(carbon nanodots) with water-induced enhanced luminescence *RSC Adv.* **6** 79620–4
- [15] Han T, Yuan Y, Liang X, Zhang Y, Xiong C and Dong L 2017 Colloidal stable quantum dots modified by dual functional group polymers for inkjet printing *J. Mater. Chem. C* **5** 4629–35
- [16] Sagara Y and Kato T 2011 Brightly tricolored mechanochromic luminescence from a single-luminophore liquid crystal: reversible writing and erasing of images *Angew. Chem., Int. Ed.* **50** 9128–32
- [17] Xiong H M 2013 ZnO nanoparticles applied to bioimaging and drug delivery *Adv. Mater.* **25** 5329–35
- [18] Kachynski A V, Kuzmin A N, Nyk M, Roy I and Prasad P N 2008 Zinc oxide nanocrystals for nonresonant nonlinear optical microscopy in biology and medicine *J. Phys. Chem. C* **112** 10721–4
- [19] Tang X, Choo E S G, Li L, Ding J and Xue J 2010 Synthesis of ZnO nanoparticles with tunable emission colors and their cell labeling applications *Chem. Mater.* **22** 3383–8
- [20] Chakrabarti S and Dutta B K 2004 Photocatalytic degradation of model textile dyes in wastewater using ZnO as semiconductor catalyst *J. Hazard Mater.* **112** 269–78
- [21] Xu T, Zhang L, Cheng H and Zhu Y 2011 Significantly enhanced photocatalytic performance of ZnO via graphene hybridization and the mechanism study *Appl. Catal. B* **101** 382–7
- [22] Yang J L, An S J, Park W I, Yi G C and Choi W 2004 Photocatalysis using ZnO thin films and nanoneedles grown by metal-organic chemical vapor deposition *Adv. Mater.* **16** 1661–4
- [23] Xu X, Xu C and Hu J 2014 High-performance deep ultraviolet photodetectors based on ZnO quantum dot assemblies *J. Appl. Phys.* **116** 103105
- [24] Guo D Y, Shan C X, Qu S N and Shen D Z 2014 Highly sensitive ultraviolet photodetectors fabricated from ZnO quantum dots/carbon nanodots hybrid films *Sci. Rep.* **4** 7469
- [25] Liu J S, Shan C X, Li B H, Zhang Z Z, Yang C L, Shen D Z and Fan X W 2010 High responsivity ultraviolet photodetector realized via a carrier-trapping process *Appl. Phys. Lett.* **97** 251102
- [26] Liu J S, Shan C X, Shen H, Li B H, Zhang Z Z, Liu L, Zhang L G and Shen D Z 2012 ZnO light-emitting devices with a lifetime of 6.8 h *Appl. Phys. Lett.* **101** 011106
- [27] Yang L, Liu K, Xu H, Liu W, Ma J, Zhang C, Liu C, Wang Z, Yang G and Liu Y 2017 Enhanced electroluminescence from ZnO quantum dot light-emitting diodes via introducing Al_2O_3 retarding layer and $\text{Ag}@\text{ZnO}$ hybrid nanodots *Adv. Opt. Mater.* **5** 1700493
- [28] Pan J, Chen J, Huang Q, Khan Q, Liu X, Tao Z, Zhang Z, Lei W and Nathan A 2016 Size tunable ZnO nanoparticles to enhance electron injection in solution processed QLEDs *ACS Photon.* **3** 215–22
- [29] Modepalli V, Jin M J, Park J, Jo J, Kim J H, Baik J M, Seo C, Kim J and Yoo J W 2016 Gate-tunable spin exchange interactions and inversion of magnetoresistance in single ferromagnetic ZnO nanowires *ACS Nano* **10** 4618–26
- [30] Aras M and Kılıç Ç 2018 Electrical tuning of spin splitting in Bi-doped ZnO nanowires *Phys. Rev. B* **97** 035405
- [31] Wang Y X, Shen Z C, Huang D D and Yang Z S 2018 High-performance ZnO nanosheets/nanocrystalline aggregates composite photoanode film in dye-sensitized solar cells *Mater. Lett.* **214** 88–90
- [32] Law M, Greene L E, Johnson J C, Saykally R and Yang P 2005 Nanowire dye-sensitized solar cells *Nat. Mater.* **4** 455–9
- [33] Zhang Z, Xu M, Liu L, Ruan X, Yan J, Zhao W, Yun J, Wang Y, Qin S and Zhang T 2018 Novel $\text{SnO}_2@\text{ZnO}$ hierarchical nanostructures for highly sensitive and selective NO_2 gas sensing *Sensors Actuators B* **257** 714–27
- [34] Wan Q, Li Q H, Chen Y J, Wang T H, He X L, Li J P and Lin C L 2004 Fabrication and ethanol sensing characteristics of ZnO nanowire gas sensors *Appl. Phys. Lett.* **84** 3654–6
- [35] Liu K K, Shan C X, He G H, Wang R Q, Dong L and Shen D Z 2017 Rewritable painting realized from ambient-sensitive fluorescence of ZnO nanoparticles *Sci. Rep.* **7** 42232
- [36] Liu K K, Shan C X, He G H, Wang R Q, Sun Z P, Liu Q, Dong L and Shen D Z 2017 Advanced encryption based on fluorescence quenching of ZnO nanoparticles *J. Mater. Chem. C* **5** 7167–73
- [37] Hadia N M A, García-Granda S and García J R 2014 Effect of the temperature on structural and optical properties of zinc oxide nanoparticles *J. Nanosci. Nanotechnol.* **14** 5443–8
- [38] Liu K K, Shan C X, Zhou R, Zhao Q and Shen D Z 2017 Large-scale synthesis of ZnO nanoparticles and their application as phosphors in light-emitting devices *Opt. Mater. Express* **7** 2682